NEUTRAL CURRENTS: EXPERIMENTAL RESULTS AT HIGH AND INTERMEDIATE ENERGIES

M. STROVINK
Physics Department and Lawrence Berkeley National Laboratory,
University of California, Berkeley, CA 94720, USA

Results from experiments at high and medium energies that are relevant to electroweak neutral currents are briefly reviewed. The most recent (1997) HERA data do not confirm the high-Q^2 excesses observed earlier there. Evidence is not found for first-generation leptoquarks with mass below $\approx$ 220 GeV, scalar or vector, with $\beta = 1$ or 0.5, independent of eq coupling; anomalous $ZZ\gamma$ or $Z\gamma\gamma$ couplings; Z' masses below $\approx$ 600 GeV, or a Z-Z' mixing angle above $\approx$ 2 mrad; or contact interactions involving fermions $qqqq$, $llqq$, $eeqq$, $\nu\nu qq$, $\nu\nu e\mu$, or $eell$, with LL, $LL+RR$, LR, $LR+RL$, $LL-LR$, VV, or AA couplings, at scales below $\approx$ 2-10 TeV.

1 Introduction

I was asked by the organizers of this conference to provide a brief review [a] of experimental results obtained at high and medium energies that are related to electroweak neutral currents. Because the audience was composed primarily of physicists focused on processes studied at lower energies or without accelerators, I chose to interpret this charge broadly. For example, I summarize the experimental limits on contact interactions without restricting the charges of the four participating fermions. As another example, in connection with the excess of high Q^2 events observed at HERA, I discuss very briefly the evidence against and for the existence of a corresponding high-E_T excess in dijet production at the Tevatron. My chief aim was to show the data, where practical, and to quote the limits on phenomena beyond the Standard Model (SM); I expose the phenomenology only where necessary to clarify an experimental plot or table. For more depth in that area I refer the reader to the SM status report by P. Langacker [1] and to the theory talk on neutral current interactions by D. Zeppenfeld. [2]

A corresponding plenary presentation on charged currents was given by Y. Sirois. [3] In deference to his expertise as an H1 participant, my own discussion of HERA deep-inelastic results is very brief. Likewise, in view of the parallel session talk by S. Schlenstedt [4] on contact interaction limits at HERA, I omit the newest H1 limits in my summary of contact interactions.

The figures and text in this written contribution are essentially unchanged

[a] www links to this contribution and the corresponding presentation may be found at `http://www-d0.fnal.gov/~strovink/`

from those in the transparencies, which were prepared in May 1998. In particular, almost all of the numbers and references have not been updated since that time. As analyses by competing experiments with similar capabilities continue to evolve, *e.g.* at LEP, HERA, and Fermilab, it should be understood that differences in experimental sensitivity that are revealed by any particular snapshot may be temporary. Except where journal references are provided, all results are preliminary.

I begin with a brief update on high Q^2 events at HERA, followed by the above mentioned short discussion on high E_T jets at the Tevatron. A possible explanation of the original H1 excess might have been provided by the existence of first-generation leptoquarks of mass ≈ 200 GeV; I present Tevatron data that essentially rule out this possibility, independent of the unknown lepton-quark coupling. After a brief discussion of Tevatron searches for anomalies at the $ZZ\gamma$ and $Z\gamma\gamma$ vertex, I turn to the main topic: limits on Z' mass and mixing in extended gauge models that are set by Tevatron, LEP, and other data. I finish by tabulating limits from many experiments on four-fermion contact

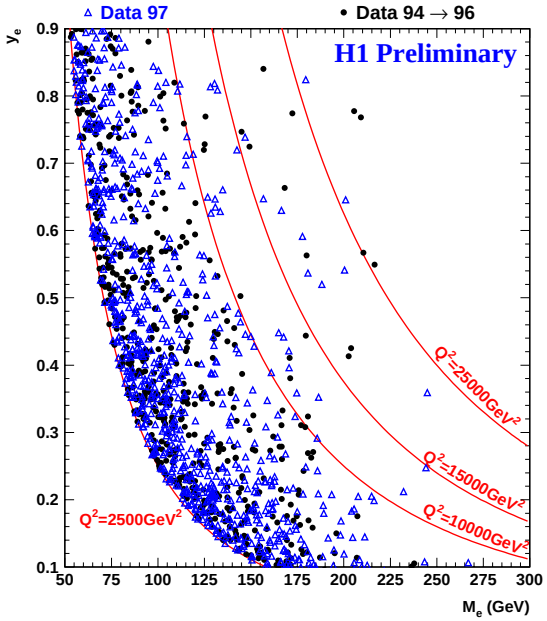

Figure 1: Distribution of NC e^+p scattering events from H1 in $y = Q^2/M^2$ and $M = \sqrt{sx_{\rm Bj}}$, collected before (•) and during (▵) 1997.

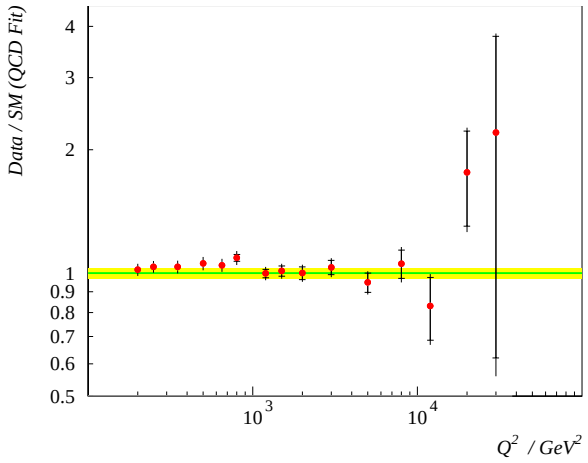

Figure 2: Ratio *vs.* Q^2 of $d\sigma/dQ^2$ from data to that from a QCD NLO fit evolved from lower Q^2 data, for the full H1 1994-97 dataset. Inner errors are statistical and outer errors are statistical+systematic added in quadrature. The shaded band is the overall luminosity error, which does not contribute to the error bars.

interactions for a variety of vector couplings.

2 Update on High Q^2 Events at HERA

In early 1997, H1 [5] and ZEUS [6] reported excesses of high Q^2 neutral current (NC) events with respect to SM expectations. The two samples of extra events

Table 1: Expected and observed totals of neutral and charged current e^+p scattering events with $Q^2 > Q^2(\text{min})$, from full 1994-97 HERA datasets.

	------ **H1** ------			---- **ZEUS** ----		
Q^2(min)			*Neutral Currents*			
(GeV/c)^2	expected	observed	P($\geq N_{obs}$)	expected	observed	P($\geq N_{obs}$)
5000	336	322	0.560	396±24	440	
10000	55	51	0.600	60±4	66	
15000	14.7±2.1	22	0.059	17±2	20	
20000	4.4±0.7	10	0.018			
25000	1.6±0.3	6	0.006			
35000				0.29±0.02	2	~ 0.035
			Charged Currents			
15000	5.1±2.8	9		3.9±1.9	8	

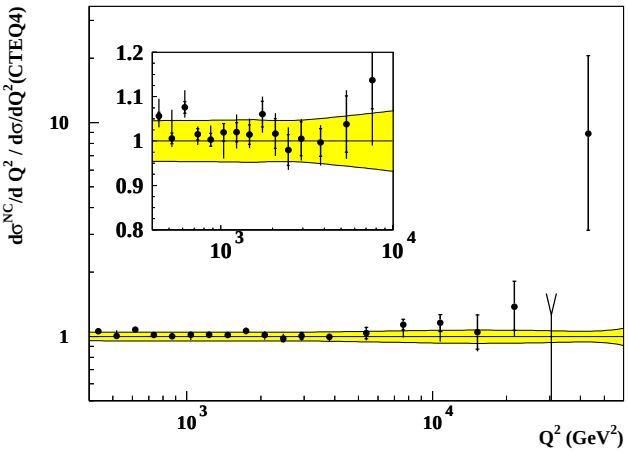

Figure 3: Ratio *vs.* Q^2 of $d\sigma/dQ^2$ from data to that from a QCD NLO fit evolved from lower Q^2 data, for the full ZEUS 1994-97 dataset. Inner errors are statistical and outer errors are statistical+systematic in quadrature. The shaded band shows the effect of varying the parton density function.

appeared, respectively, in two disjoint regions of electron-jet invariant mass M_{ej}; the H1 excess was clustered near $M_{ej} = 200$ GeV ($\bullet$ in Fig. 1). The fluctuation probabilities were of order 1%. Data collected in 1997 by H1 [7] (Δ in Fig. 1), and by ZEUS [8], did not confirm these excesses.

The full 1994-97 H1 (Fig. 2) and ZEUS (Fig. 3) preliminary datasets, when compared to expectations for deep inelastic scattering, show residual excesses at highest Q^2. These are summarized in Table 1, where it should be noted that the entries are cumulative and therefore not all independent. The significances of these excesses are reduced compared to those for the 1994-96 data alone.

The high x HERA NC data match smoothly to structure functions determined by ep and μp scattering in fixed target experiments. Shown in Fig. 4 is the current H1 determination of σ (equal to the cross section differential in x and Q^2, multiplied by kinematic factors so that $\sigma = F_2$ if F_L, and the parity violating term F_3 from Z^0 exchange, are ignored). Observed are the expected γZ interference and high-x nonscaling. Including the full H1 dataset in an NLO QCD fit pulls σ *below* the high-Q^2 extrapolation of an MRSH fit to fixed target data – not an excess!

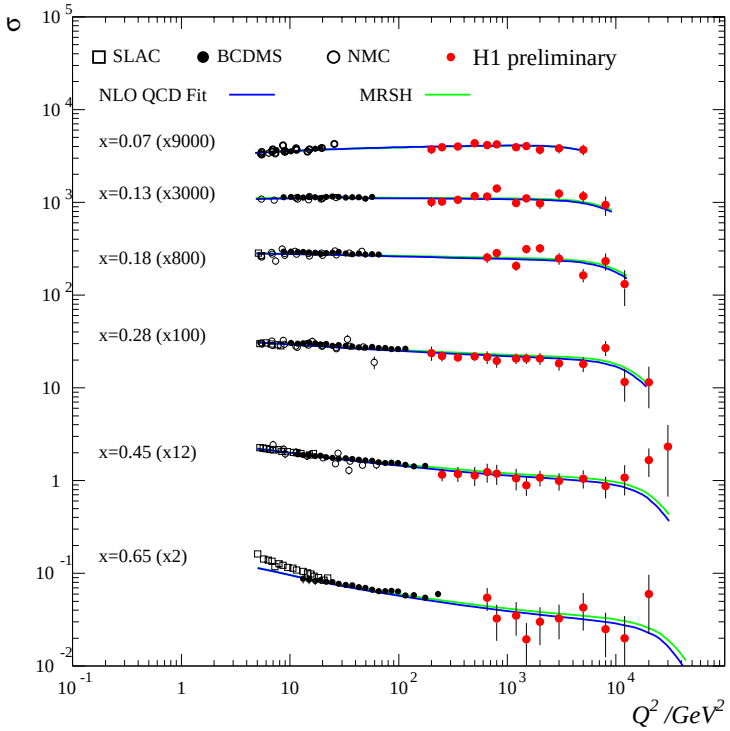

Figure 4: σ (see text) *vs.* Q^2 for 1994-97 H1 neutral current e^+p scattering data (filled circles at high Q^2) with $x_{\rm Bj}$ as parameter, compared with the extrapolation of an MRSH fit (light line) to fixed target data (other points). The heavy line is an NLO QCD fit to all points.

3 Is a Corresponding High-E_T Excess Seen in $p\bar{p}$ Collisions?

Shown at the top of Fig. 5 are CDF's (data-CTEQ3M)/CTEQ3M points, from 1992-93 (published, ○) [9] and 1994-95 (preliminary, ●) [10] data. Errors are statistical. CDF concludes that standard parton density functions (PDFs), like CTEQ3M, require modification. These authors provide an analytic function that passes smoothly through their data points.

In the lower part of Fig. 5, DØ's 1994-95 data [11] are compared to standard PDFs and also to CDF's analytic function. The systematic error bands are parametrized by a covariance matrix, allowing a χ^2 to be calculated. The standard PDFs give acceptable χ^2 values, but the χ^2 probability for CDF's analytic function is of order 10^{-5}.

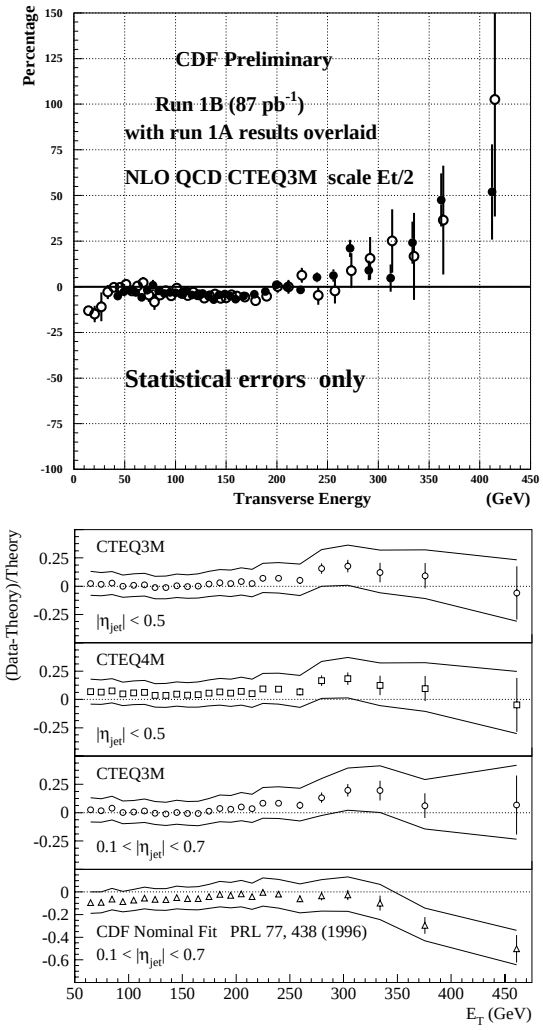

Figure 5: (Top) Percentage difference between the inclusive jet cross section from 1992-93 CDF data (open points) or preliminary 1994-95 CDF data (filled points) and a NLO EKS calculation using the CTEQ3M′ PDF with $\mu = \frac{1}{2}E_T^{\rm jet}$. Errors are statistical. (Bottom, first three panels) Fractional difference (points) between the inclusive jet cross section from 1994-95 DØ data and a NLO JETRAD calculation for the indicated PDFs, averaged over the indicated pseudorapidity ranges, with $\mu = \frac{1}{2}E_T^{\rm max}$. Errors are statistical; lines show the $\pm 1\sigma$ systematic uncertainties. (Bottom, last panel) Fractional difference between DØ data and an analytic curve passing smoothly through the CDF data.

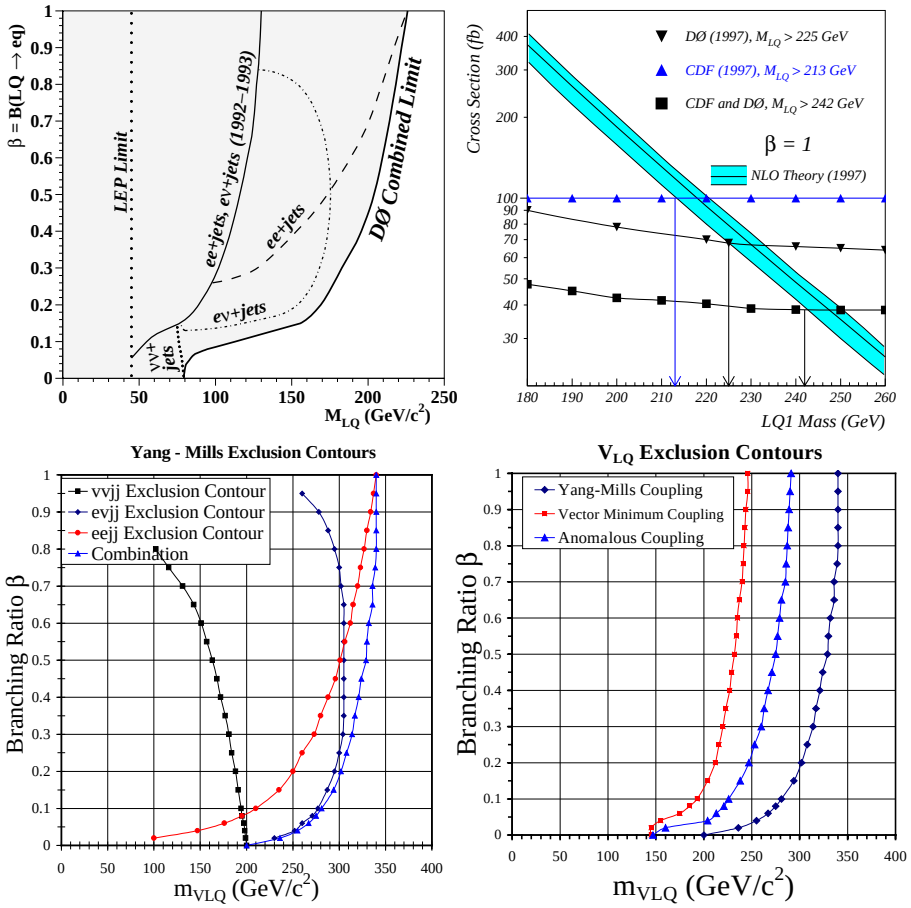

Figure 6: (Top left) Contours of $\beta \equiv \mathrm{BR}(\mathrm{LQ}_1 \to eq)$ *vs.* $M(\mathrm{LQ}_1)$ for first generation scalar leptoquarks. The shaded region is excluded by DØ ee+jets, $e\nu$+jets, and $\nu\nu$+jets data. (Top right) NLO cross section for $p\bar{p} \to \mathrm{LQ}_1\mathrm{LQ}_1 X$ vs. $M(\mathrm{LQ}_1)$ (band). 95% confidence upper limits are shown for DØ (∇), CDF (Δ), and combined ($\Box$) data. (Bottom left) DØ limits, as at top left, for Yang-Mills vector leptoquark coupling. (Bottom right) Combined DØ exclusion contour, as at bottom left, for three different vector couplings.

4 Limits on First-Generation Leptoquarks

If first-generation leptoquarks (LQ_1s) were to exist, the new interaction that would bind e to q would enhance eq scattering near the LQ_1 mass (≈ 200 GeV, suggested by 1994-96 H1 data). At the Tevatron, LQs could be pair produced

strongly, independent of the lepton-quark coupling. Shown at top left in Fig. 6 is DØ's published [12] scalar LQ_1 mass limit *vs.* $\beta \equiv \mathrm{BR}(LQ_1 \to eq)$. For $\beta = 1$, $M(LQ_1) > 225$ GeV. Additional points from CDF [13] limit $M(LQ_1) > 213$ (180) GeV for $\beta = 1$ (0.5). At top right in Fig. 6, DØ and CDF combine their $(LQ_1 \to eq)$ searches to limit $M(LQ_1) > 242$ GeV for $\beta = 1$.

Recently DØ completed a similar search [14] for vector leptoquark pair production. As in the scalar case, the combined limit contours *vs.* β are the result of separate analyses in the $eejj$, $e\nu jj$, and $\nu\nu jj$ channels (Fig. 6 bottom left). The DØ combined limit contours are presented (Fig. 6 bottom right) for three choices of vector coupling. The "minimum" coupling yields the smallest possible vector LQ_1 production rate. Even for minimum vector coupling, the mass limit contour is more stringent than for the scalar case.

5 Limits on Anomalous $ZZ\gamma$ and $Z\gamma\gamma$ Couplings

In the SM, both the $ZZ\gamma$ and $Z\gamma\gamma$ couplings vanish. CP-conserving anomalous $ZV\gamma$ couplings h_{30}^V and h_{40}^V correspond to the E1 and M2 transition moments of the $ZV\gamma$ vertex, where V is either Z or γ. To satisfy unitarity, they are multiplied by $(1 + \bar{s}/\Lambda^2)^{-n}$, where n is h's first subscript. Shown at the top of Fig. 7 are DØ's combined limits [15] on h_{30}^V and h_{40}^V. At the bottom are the data [16] which mainly limit these anomalous couplings – the non-observation by DØ, above background and SM radiative effects, of $Z\gamma$ production in which $Z \to \nu\nu$, yielding a γ + missing energy signature.

6 Limits on Z' Mass and Mixing in Extended Gauge Models

New heavy gauge bosons are expected if the Standard Model is extended by additional gauge symmetries. These extensions are motivated *e.g.* by grand unified theories (GUTs) or by compactified string models. An example is the decomposition

$$E6 \to U(1)_\psi \times SO(10) \to U(1)_\psi \times U(1)_\chi \times SU(5) \to U(1)_{\theta_{E6}} \times \mathrm{SM}$$

The Z' boson originating from this new $U(1)$ symmetry is labeled by the angle θ_{E6} by which $U(1)_\psi$ mixes with $U(1)_\chi$ mix to form it. Often-studied cases [17] are

$$\begin{aligned}
\theta_{E6} &= 0 && \text{(model ``}\chi\text{'')} \\
&= \pi/2 && \text{(model ``}\psi\text{'')} \\
&= \arctan(-\sqrt{5/3}) && \text{(model ``}\eta\text{'')} \\
&= \arctan(\sqrt{15}) && \text{(model ``}\nu\text{'')}
\end{aligned}$$

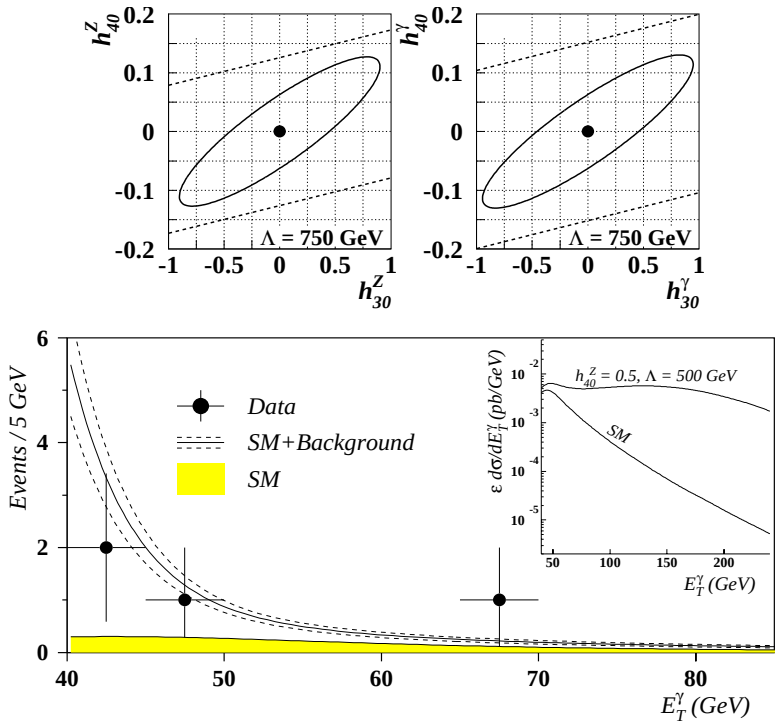

Figure 7: (Top) Combined 95% confidence limits from DØ data on h_{30}^V and h_{40}^V, the anomalous E1 and M2 transition moments of the $ZV\gamma$ vertex. At left, $V = Z$; at right, $V = \gamma$. Ellipses shows the 95% CL limit and bands show the unitarity constraint. (Bottom) Distribution of γ transverse energy for DØ events consistent with $p\bar{p} \to \gamma Z\, X \to \gamma\nu\nu\, X$. The inset shows the expectation from an anomalous $h_{40}^Z = 0.5$.

The Z'-fermion couplings for these models are prescribed within a range, with the upper bound usually taken. As another example, the left-right model [18]

$$SO(10) \to U(1)_{B-L} \times SU(2)_R \times SU(2)_L \times SU(3)_C \quad \text{(model "LR")}$$

has a Z' with fermion couplings fixed by manifest left-right symmetry. Another ("ALR") left-right model [18] originates from $E6$ GUTs. It has a nonstandard W_R and different Z'-fermion couplings. Finally, experimenters often refer to a toy "SSM" model in which the Z' couplings are identical to those of the Z.

The above described models *fail* [19] to span a reasonable set of possibilities:

- Kinetic mixing can shift the couplings. Its term in the Lagrangian has a factor $\sin\chi$, which these models take to be zero.

- String theorists describe a broader class of models with additional $U(1)$ factors.

At the (physical) Z_1 pole, e^+e^- experiments are sensitive mainly to the presence of a mixing angle θ_M between the (SM) Z and the Z', yielding the Z_1. [Specific assumptions involving the Z-Z' mass matrix allow limits on θ_M to be re-expressed as limits on M(Z') when $M(Z') \gg M(Z)$.] The chief experimental constraints at the Z_1 pole are the hadron- and lepton-pair cross sections and the lepton forward-backward and left-right asymmetries. When cross sections and forward-backward asymmetries well above the Z_1 pole from LEP 2 are included, sensitivity independently to both θ_M and $M(Z')$ is achieved.

6.1 Z' Mass and Mixing Limits from LEP

L3 make a fit[20] to their LEP1 and LEP2 cross sections and lepton asymmetries, using ZEFIT, an extension to ZFITTER. Preliminary limits at 95% CL in the $\theta_M - M(Z')$ plane are obtained for the χ, ψ, η, and LR models as exhibited in Fig. 8. The L3 limits on θ_M are competitive with recent fits to world data. However, except for the toy "SSM" model, for which they obtain $M(Z') > 805$ GeV, L3 limits on $M(Z')$ are not as strong as those available from Tevatron searches.

6.2 Z' Mass and Mixing Limits from the Tevatron

At the Tevatron, direct searches for $Z' \to e^+e^-$ and $\mu^+\mu^-$ yield limits on $M(Z')$ that do not vary widely among the various models. Displayed in Fig. 9 are the $\sigma \times B$ limits from CDF[21] as a function of dilepton mass (top), and from DØ[22] as a function of dijet mass (bottom). The latter constrains a possible "leptophobic" Z' with SM couplings to quarks.

For comparison with Fig. 8, the CDF and DØ Z' mass limits are displayed on the same scale in Fig. 10. CDF's $M(Z')$ limits (top left) for a variety of models are published; the areas beneath the lines are excluded. DØ's Z' searches (top right) are preliminary. The region between the "leptophobic" dashed lines is excluded by nonobservation of a bump in DØ's dijet mass spectrum.

6.3 Z' Mass and Mixing Limits from Global Fits

Except for the toy "SSM" case, the Tevatron mass limits are stronger than those obtained from recent fits to all indirect constraints, including low-energy weak neutral current processes. Exhibited in Fig. 10 (bottom left) is the result

of Cvetič and Langacker's 1997 fit [17] to all available data, excluding direct Tevatron searches and LEP 2 data, but including low-energy constraints that are outside the scope of this review. (Plotted is the rectangle within which their limiting contour could be inscribed.) The $M(Z')$ limits are for the case in which no assumption is made on the $U(1)'$ charges. In the χ and LR models, respectively, if definite $U(1)'$ charges are assumed, much higher minimum Z' masses of 1160 and 1680 GeV are obtained.

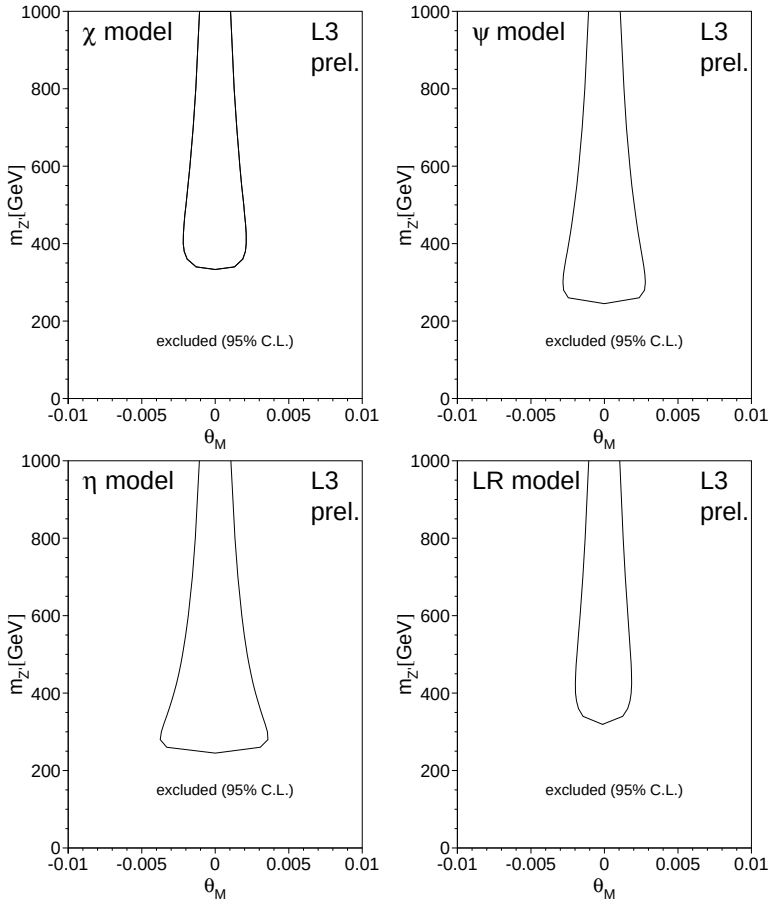

Figure 8: 95% confidence limits on $M(Z')$ *vs.* Z-Z' mixing angle θ_M from cross sections and lepton asymmetries measured by L3 at LEP1 and LEP2, for four extended gauge models described in the text. The areas outside the contours are excluded.

Plotted likewise in Fig. 10 (bottom right) are the results of the more general May 1998 fit of Cho, Hagiwara, and Umeda [23] to data similar to those used

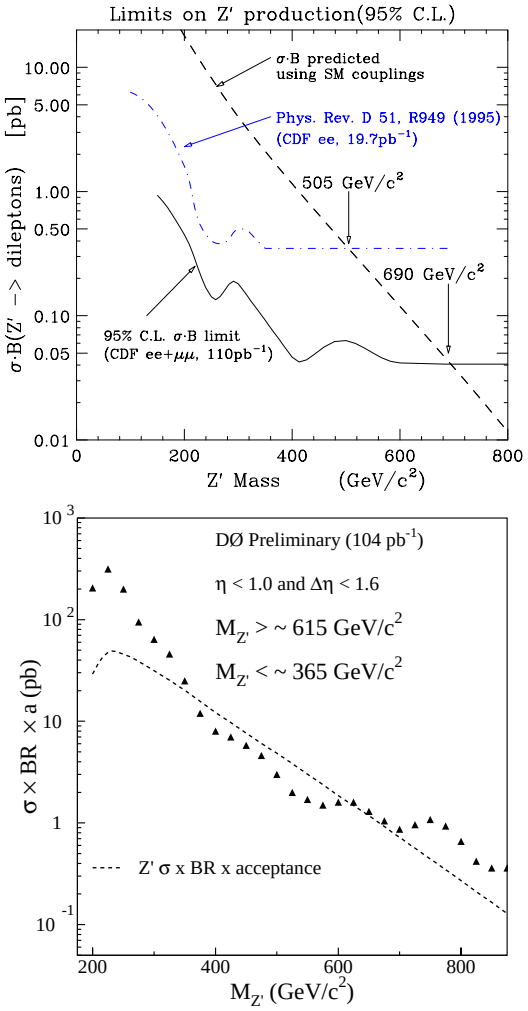

Figure 9: (Top) 95% confidence limits from 1994-95 and 1992-93 CDF data on $\sigma(p\bar{p} \to Z'X) \times \mathrm{BR}(Z' \to ee, \mu\mu)$ *vs.* $M(Z')$. The dashed line is the SSM model prediction (see text). (Bottom) 95% confidence limit from 1994-95 DØ data on $\sigma(p\bar{p} \to Z'X) \times \mathrm{BR}(Z' \to qq) \times$ acceptance *vs.* $M(Z')$. The dashed line is the expectation assuming SM coupling of Z' to quarks.

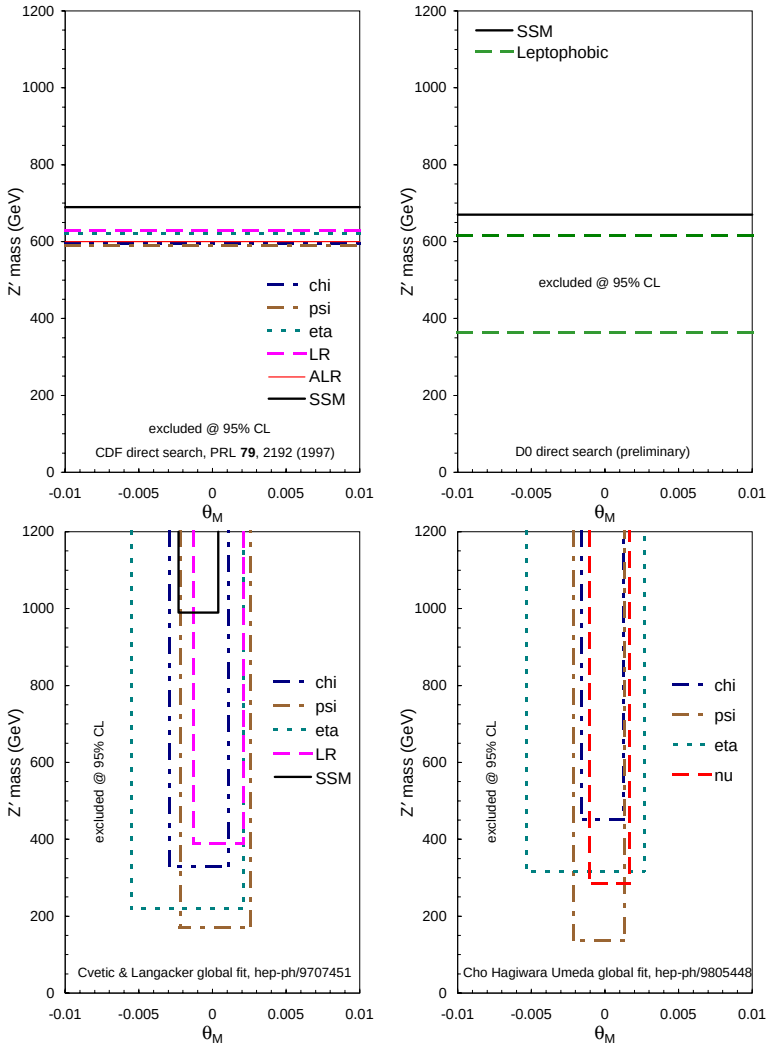

Figure 10: 95% confidence limits on $M(Z')$ *vs.* Z-Z' mixing angle θ_M for extended gauge models described in the text. (Top left) Upper limits on $M(Z')$ from CDF's direct search for $Z' \to e^+e^-$ and $\mu^+\mu^-$ (Fig. 9 top). (Top right) Limits on $M(Z')$ from DØ's direct search for $Z' \to e^+e^-$ (solid line) and for $Z' \to qq$ (Fig. 9 bottom) (region within dashed lines is excluded). (Bottom) Limits from global fits by (left) Cvetič and Langacker and (right) Cho, Hagiwara, and Umeda to measurements sensitive indirectly to $M(Z')$ and θ_M. Contours enclosing the allowed regions would be inscribed within the rectangles that are shown.

by Cvetič and Langacker. To put this plot on the common scale, Cho *et al.*'s mixing angle limits are divided by $(\sqrt{5/3} \times \sin\theta_W)$. If definite U(1)$'$ charges are assumed and other parameters are varied, lower limits on the Z' mass are obtained for all models. Compared to those in the plot, most of these mass limits are far stronger, of order 1-2 TeV. However, these are still below the LHC discovery limits (≈ 3 TeV).

We mention briefly the inputs and method of Cho *et al.* Their first fit uses the results of Z-pole experiments together with measurements of $M(W)$, $m(t)$, α_s, and α. It constrains mainly the Z-Z' mixing angle θ_M and the T parameter. Their second fit adds low-energy neutral current measurements. Sensitivity to the Z' mass through a contact term is gained, along with modest improvement in constraints on the other parameters.

7 Limits on Contact Interactions

At $s \ll M^2(Z')$, Z' exchange would represent one form of effective four-fermion contact interaction. The scale Λ of the contact interaction parametrizes searches for quark and lepton compositeness. The vector contact Lagrangian [34] has terms of the form

$$\eta_{HH'}(\bar{f}_H\gamma_\mu f_H)(\bar{f}'_{H'}\gamma^\mu f'_{H'})$$

where $fff'f'$ are the four fermions involved, H and H' run over chiralities $\{L, R\}$, and $\eta = 4\pi/\Lambda^2$. [Tensor $eeff$ contact interactions with $\Lambda < 130$ TeV and scalar $eeee$ contact interactions with $\Lambda < 45$ TeV are ruled out by electron dipole moment limits, and tensor $qq\mu\mu$ or $\mu\mu\tau\tau$ contact interactions with $\Lambda < 16$ TeV are ruled out by muon $(g-2)$ measurements. Therefore high energy experiments focus mainly on vector terms.]

Table 2 presents typical experimental limits on vector contact interactions involving fermions $qqqq$, $llqq$, $eeqq$, $\nu\nu qq$, $\nu\nu e\mu$, and $eell$, where q (l) assigns the same contact interaction to all quarks (charged leptons). For each fermion set, the limits are described further by the assumed relative magnitudes of the coefficients $(\eta_{LL}, \eta_{LR}, \eta_{RL}, \eta_{RR})$. We consider the cases LL $(1,0,0,0)$, $LL+RR$ $(1,0,0,1)$, LR $(0,1,0,0)$, $LR+RL$ $(0,1,1,0)$, $LL-LR$ $(1,-1,0,0)$, VV $(1,1,1,1)$, and AA $(1,-1,-1,1)$. (Typically the limits for RR (RL) [$RL-RR$] are similar to those for LL (LR) [$LL-LR$].) Lower limits $\Lambda+$ and $\Lambda-$ are set at 95% confidence (single-sided) on the energy scale for each case, corresponding to whether the first nonvanishing η is positive or negative. Atomic parity violation experiments place severe constraints [$\Lambda > \mathcal{O}(10$ TeV)] on Lagrangians for which the sum $\eta_{LL} + \eta_{LR} - \eta_{RL} - \eta_{RR}$ does not vanish. Therefore the cases LL and LR are included in Table 2 only for the purpose of comparing experimental sensitivities.

Table 2: Typical experimental lower limits $\Lambda+$ and $\Lambda-$ (see text) on the mass scale of vector contact interactions among four fermions (first column) with the chiralities shown in the heading (see text). Limits from DØ, [24,25] CDF, [26] OPAL, [27] L3, [28] ALEPH, [29] ZEUS, [30] CCFR, [31] and TRIUMF E185 [32] data and from fits by Gonzalez-Garcia *et al.* [33] and Barger *et al.* [34] are tabulated.

chirality		***LL*** ♣♥		***LL+RR***		***LR*** ♥♣		***LR+RL***		***LL−LR*** ♥♥		***VV***		***AA***	
95% scale (TeV)		Λ+	Λ−	Λ+	Λ−	Λ+	Λ−	Λ+	Λ−	Λ+	Λ−	Λ+	Λ−	Λ+	Λ−
qqqq	D0	**2.1**	**1.9**												
	CDF	1.8	1.6												
llqq	CDF	3.1	**4.3**			3.3	**3.9**					**5.0**	**6.3**	4.5	**5.6**
eeqq	D0♠	3.3	**4.2**			**3.4**	**3.6**					**4.9**	**6.1**	4.7	**5.5**
	CDF	2.5	3.7			2.8	3.3					3.5	5.2	3.8	4.8
	OPAL 183♠	**4.4**	2.8	**4.4**	**3.8**	3.3	**3.6**	3.1	**5.5**			4.1	5.7	**6.3**	3.8
	L3 172	3.0	2.1	3.2	2.8	2.4	2.6	2.4	3.7			3.2	3.9	4.3	2.9
	ALEPH 183♠	3.9	2.7	4.1	3.6	2.1	3.4	3.0	4.9			4.0	5.2	5.6	3.7
	ZEUS♠			2.8	1.5			**4.5**	4.1	1.8	3.0	**4.9**	4.6	2.0	4.0
	Gonzalez *et al*	3.3	3.7	3.0	3.4	3.4	3.0	3.0	2.7			1.1	1.2	4.3	4.8
	Barger *et al*							3.5	5.3	3.5	3.8	4.1	6.9	4.4	4.7
$\nu\nu$ ***qq***	CCFR	4.7	5.1			4.2	4.4					8.0	8.3	3.7	5.9
$\nu\nu$ ***e*** μ	TRIUMF E185					3.1♦		3.1♦		3.1♦					
eell	OPAL 183♠	5.2	5.3	7.2	7.4	5.6	**5.2**	7.8	7.3			9.6	9.3	7.7	8.3
	L3 172	4.0	3.1	5.5	4.4	3.4	4.0	4.8	4.3			7.1	5.8	4.9	4.1
	ALEPH 183♠	**6.1**	**5.4**	**8.4**	**7.5**	**6.5**	**5.2**	**9.4**	**7.4**			**11.8**	**9.4**	**8.2**	**9.0**

♦***RR*** typically similar. ♥♥***RL*** typically similar. ♥♥***RL*** **–*RR*** typically similar.

♣Severe atomic parity violation constraints exist. ♠Preliminary. ♦If $\nu_R > 20$ MeV/c^2 or nonexistent.

Gonzalez-Garcia, Gusso, and Novaes (hep-ph/9802254) obtain limits from LEP/SLD $\Gamma_l(Z)$ using a one-loop calculation.

Barger, Cheung, Hagiwara and Zeppenfeld (hep-ph/9707412) fit mid '97 world data at low, medium, and high energies.

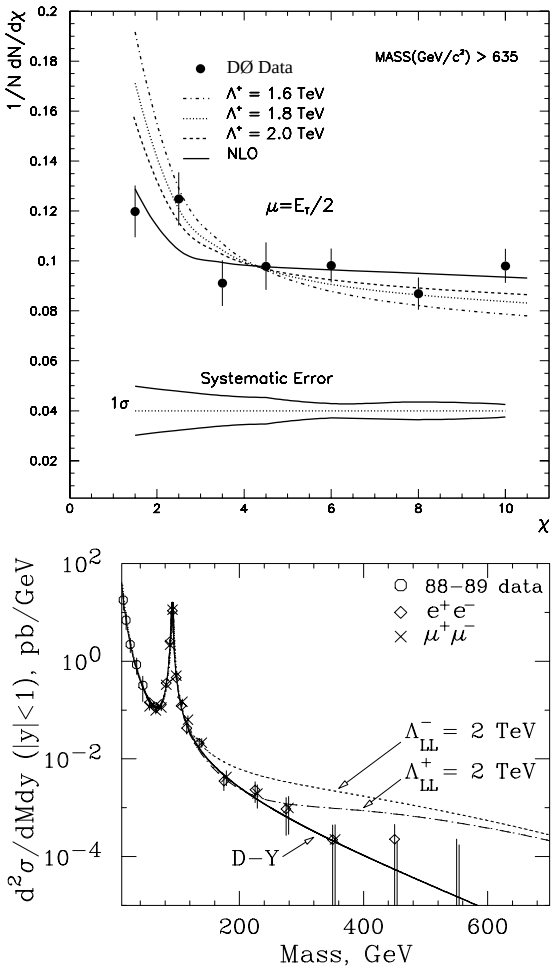

Figure 11: (Top) Angular distribution (see text) of DØ dijet data with $M_{jj} > 635$ GeV/c^2 *vs.* NLO JETRAD prediction, showing the central ($\chi \to 1$) enhancement that would be expected if $\Lambda^+_{LL}(qqqq) = 2$ TeV. (Bottom) Invariant mass distribution of CDF e^+e^- and $\mu^+\mu^-$ pairs *vs.* Drell-Yan prediction, showing the high-mass enhancement that would be expected if $\Lambda^\pm_{LL}(llqq) = 2$ TeV.

7.1 Contact-Interaction Limits from the Tevatron

We conclude this brief discussion of limits on contact interactions by displaying a few of the inputs from high-energy experiments. The best limits on quark

compositeness ($qqqq$) result from DØ's measurement [24] of the dijet angular distribution, shown in Fig. 11 (top). Rutherford scattering is flat in the variable χ ($\chi = 1$ when $\theta^* = 90°$). Contact interactions would be more central than t-channel gluon exchange, resulting in an enhancement near $\chi = 1$.

Important constraints on quark-lepton compositeness ($llqq$) result from DØ's [25] and CDF's [26] studies of Drell-Yan ee and $\mu\mu$ production. The CDF data are shown at the bottom of Fig. 11. For the limits listed in Table 2, contact-interaction couplings to u and d quarks are assumed to be equal. From these same CDF data, a limit $\Lambda > 3.3$ GeV on the scale of *llqq scalar* couplings is also obtained.

7.2 Contact-Interaction Limits from LEP

At tree level at the Z_1 pole, (real) contact interactions do not interfere with (imaginary) electroweak processes, so experiments are insensitive to them. At one-loop level [33], contact interactions do affect the leptonic Z width. Above the Z_1 pole, especially including 183 GeV data such as those from ALEPH [29] shown in Fig. 12, fermion pair cross sections (left) and angular distributions (A_{FB}, right) strongly limit the $eeqq$ and $eell$ contact interaction scales.

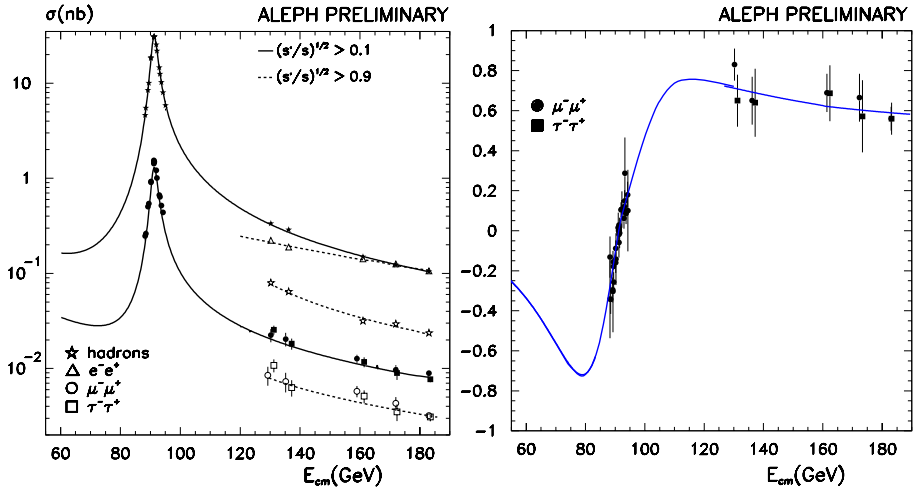

Figure 12: Cross section (left) and forward-backward asymmetry A_{FB} (right) *vs.* $\sqrt{s}$ for ALEPH dilepton and hadron data, compared to SM expectations. These and similar LEP1/LEP2 data strongly constrain $\Lambda(eell)$ and $\Lambda(eeqq)$.

Conclusions

The most recent (1997) HERA data do not confirm the high-Q^2 excesses observed earlier there. So far, evidence is not found for:

- First-generation leptoquarks with mass below ≈ 220 GeV, scalar or vector, with $\beta = 1$ or 0.5, independent of eq coupling.
- Anomalous $ZZ\gamma$ or $Z\gamma\gamma$ couplings.
- Z' masses below ≈ 600 GeV, or a Z-Z' mixing angle above ≈ 2 mrad.
- Contact interactions involving fermions $qqqq$, $llqq$, $eeqq$, $\nu\nu qq$, $\nu\nu e\mu$, or $eell$, with LL, $LL+RR$, LR, $LR+RL$, $LL-LR$, VV, or AA couplings, at scales below $\approx$ 2-10 TeV.
- Many other possible new physics signals not addressed by this short review.

Experiments below as well as on the energy frontier continue to raise the thresholds for possible discovery of new high-mass phenomena.

Acknowledgements

I am grateful to C. Kolda and P. Langacker for discussions, and to my experimental colleagues, particularly in the DØ group, for making their data available. I thank C.M. Hoffman, P. Herczeg, and the Organizing Committee for their kind invitation to this superb conference. This work was supported by the U.S. Department of Energy under Contract No. DE-AC03-76F00098.

References

1. P. Langacker, these Proceedings.
2. D. Zeppenfeld, these Proceedings.
3. Y. Sirois, these Proceedings.
4. S. Schlenstedt, these Proceedings.
5. C. Adloff *et al.* (H1 Collaboration), Z. Phys. **C74**, 191 (1997).
6. J. Breitweg *et al.* (ZEUS Collaboration), Z. Phys. **C74**, 207 (1997).
7. B. Heinemann (H1 Collaboration), presented at DIS 98 (1998).
8. D.C. Williams (ZEUS Collaboration), presented at DIS 98 (1998).
9. F. Abe *et al.* (CDF Collaboration), Phys. Rev. Lett. **77**, 438 (1996).
10. See *e.g.* B. Flaugher for the CDF Collaboration, Fermilab-Conf-96/225-E (1996).

11. B. Abbott *et al.* (DØ Collaboration), hep-ex/9807018, submitted to Phys. Rev. Lett. (1998).
12. B. Abbott *et al.* (DØ Collaboration), Phys. Rev. Lett. **80**, 2051 (1998); *ibid*, Phys. Rev. Lett. **79**, 4321 (1997).
13. F. Abe *et al.* (CDF Collaboration), Phys. Rev. Lett. **79**, 4327 (1997); H.S. Kambara for the CDF Collaboration, presented at HCP 97 (1997), `http://sbhep1.physics.sunysb.edu/~hadron97/june07/pm-6/Writeup.ps`.
14. A. Boehnlein for the DØ Collaboration, presented at QCD Moriond 98, Fermilab-Conf-98-337-E.
15. B. Abbott *et al.* (DØ Collaboration), Phys. Rev. **D57**, 3817 (1998).
16. B. Abbott *et al.* (DØ Collaboration), Phys. Rev. Lett. **78**, 3640 (1997).
17. M. Cvetič and P. Langacker, hep-ph/9707451 (1997).
18. See *e.g.* M. Cvetič and S. Godfrey, hep-ph/9504216 (1995), and references therein.
19. See *e.g.* K.S. Babu, C. Kolda, and J. March-Russell, Phys. Rev. **D57**, 5825 (1998); *ibid*, in C. Caso *et al.* (Particle Data Group), Eur. J. Phys. **C3**, 254 (1998).
20. L3 Collaboration, L3 Note #2282 (1998), `http://l3www.cern.ch/analysis/JoachimMnich/paper_ichep/note_2282.ps`.
21. F. Abe *et al.* (CDF Collaboration), Phys. Rev. Lett. **79**, 2192 (1997).
22. B. Abbott *et al.* (DØ Collaboration), submitted to Lepton-Photon 97 (1997), Fermilab-Conf-97-356-E.
23. G.-C. Cho, K. Hagiwara, and Y. Umeda, hep-ph/9805448 (1998), to appear in Nucl. Phys. **B**.
24. B. Abbott *et al.* (DØ Collaboration), Phys. Rev. Lett. **80**, 666 (1998).
25. B. Abbott *et al.* (DØ Collaboration), Fermilab-Conf-98-273-E (1998).
26. F. Abe *et al.* (CDF Collaboration), Phys. Rev. Lett. **79**, 2198 (1997).
27. OPAL Collaboration, submitted to Eur. Phys. J. **C** (1998), CERN-EP/98-108.
28. L3 Collaboration, L3 Note #2229 (1998), `http://l3www.cern.ch/analysis/JoachimMnich/paper_ichep/note_2229.ps`; Phys. Lett. **B433**, 163 (1998). Table 2 uses the latter ($\sqrt{s} \leq 172$ GeV) reference because the limits on Λ are not tabulated in the former.
29. ALEPH Collaboration, ALEPH 98-060 (1998), `http://alephwww.cern.ch/~alephsec/hep/an906.ps`.
30. ZEUS Collaboration, submitted to ICHEP 98, `http://www-zeus.desy.de/conferences98/ichep98papers/753.ps`.
31. K.S. McFarland *et al.* (CCFR Collaboration), Eur. Phys. J. **C1**, 509 (1998).

32. A. Jodidio *et al.*, Phys. Rev. **D34**, 1967 (1986); Phys. Rev. **D37**, 237 (E) (1988).
33. M.C. Gonzalez-Garcia, A. Gusso, and S.F. Novaes, hep-ph/9802254 (1998).
34. V. Barger, K. Cheung, K. Hagiwara, and D. Zeppenfeld, Phys. Rev. **D57**, 391 (1998).